



ELSEVIER

Journal of Non-Crystalline Solids 192 & 193 (1995) 534–538

JOURNAL OF
NON-CRYSTALLINE SOLIDS

Aggregation process in silica aerogels on sintering

Nicolás de la Rosa-Fox^{*}, Luis Gago-Duport, Luis Esquivias

Departamento de Física de la Materia Condensada, Facultad de Ciencias, Universidad de Cádiz, Apartado 40, 11510 Puerto Real (Cádiz), Spain

Abstract

The ultrastructural evolution of aerogels on sintering into glass must be understood on the basis of a detailed description of a solid backbone and porosity. Silica aerogels from ‘sonogels’ have been studied over a wide length-scale range, using small-angle X-ray scattering and gas adsorption measurements. An aggregation model of a hierarchical nature can be formulated with a variable clustering index (N is the number of elementary units inside a cluster) and hierarchical ratio (size of a cluster in terms of the size of the elementary unit). The results reveal a change in the hierarchical level during the sintering process, which is ultrasonic dose-dependent.

1. Introduction

The sol–gel method is an alternative approach for making monolithic glasses [1,2]. One method for preventing cracking is to dry the wet gel under hypercritical conditions, thus obtaining a porous solid known as an ‘aerogel’. These two phase systems (porosity–solid matrix) have many specific properties, after drying and during sintering [3]. The aerogels, as porous bodies, sinter by viscous flow, causing the collapse of pores or the coalescence of solid particles. The driving force for this process is supplied by the interfacial energy, which allows sintering at low temperatures. The study of the partially sintered aerogel makes it possible to monitor the intermediate and final properties of the material [4,5].

The combined effect of high-power ultrasound and the absence of any added solvent in the liquid state gives rise to a gel made up of small and

uniformly sized particles and pores. As a consequence, the surface : volume ratio is twice as large as that for gels prepared in an alcoholic solution [6]. This property makes these gels begin to sinter at lower temperatures. The dense, cross-linked wet ‘sonogels’ are dried under hypercritical conditions to prevent any shrinkage, resulting in an aerogel whose density is 40–50% that of vitreous silica (2.2 g cm^{-3}), whereas the density of classic aerogels is about 10–20% [7,8].

This work presents the application of a geometrical model, describing the structure of aerogels as a hierarchical arrangement of spherical units clustered in successive steps [9]. The model takes into account the clustering index (number of elementary units in a cluster) and the hierarchical ratio (size of a cluster in terms of the size of the elementary unit). The structural parameters are evaluated from a chord distribution of the small-angle X-ray scattering (SAXS) results analysis for the two-phase systems and a spherical packing for the Brunauer–Emmett–Teller (BET) data. Most of the structural characteristics of

^{*} Corresponding author. Tel: +34-56 830 966. Telefax: +34-56 837 205. E-mail: rosa@galeon.uca.es.

these materials are at the resolution length scale of these experiments (1–100 nm). The model accounts for the degree of branching and the connectivity of the aerogels on sintering and the effect of the ultrasonic dose used.

2. Experimental procedures

2.1. Sample preparation and characterization

The experimental conditions for the preparation of aerogels have already been reported [10]. In this study, two series of acid-catalyzed and ultrasonically treated sonogels were used. One was obtained with a low ultrasonic dose (0.1 kJ cm^{-3}) and gelified at 50°C (L5), 0.65 g cm^{-3} being the resulting aerogel bulk density. The other was submitted to a high ultrasonic dose (0.35 kJ cm^{-3}) and the same gelation temperature (H5) with 0.82 g cm^{-3} aerogel bulk density.

After hypercritical evacuation of the interstitial liquid, the aerogels were oxidized at 500°C for 5 h and dehydrated by chlorination at 500°C for 5 h by means of a flux of nitrogen passed through CCl_4 . Both aerogel series were submitted to the same heat treatment and were taken from the same batch to ensure identical starting structures.

The specific surface area was measured through the BET method, using isothermal nitrogen adsorption (77 K). SAXS experiments were carried out using the LURE synchrotron radiation facility at Orsay, France. A high-flux, 8 keV, circular cross-section beam was used. The data were collected in the scattering vector modulus range of $q = 0.008\text{--}0.25 \text{ \AA}^{-1}$, where $q = 4\pi \sin \theta / \lambda$, 2θ is the scattering angle and λ is the X-ray wavelength.

2.2. Data analysis

Information derived from gas adsorption can be interpreted on the basis of packing spheres, so that surface area, S_{BET} decreases as particle size, l_s increases according to the relationship

$$l_s (\text{\AA}) = \frac{6 \times 10^4}{S_{\text{BET}} (\text{m}^2 \text{ g}^{-1}) \rho_{\text{skeleton}}}, \quad (1)$$

where the silica spheres have a skeletal density $\rho_{\text{skeleton}} = 2.2 \text{ g cm}^{-3}$.

The SAXS data have been analyzed by considering the aerogel as a two-phase system, comprising solid backbone plus porosity. The structural parameters were calculated through chord distribution analysis. This means the aerogel is penetrated by random test lines, which yield the pore chord, l_p , and the solid chord, l_s , as the average intersection lengths of the test lines with the voids and solid phase.

Porod's law was used to extract the information from the SAXS intensities [11]. However, the aerogels studied exhibit a positive deviation from this law due to electronic density fluctuation at the pore-solid boundary. In this case, it is necessary to represent the intensity as

$$Iq^4 = A + Bq^4,$$

in the high q -region by [12], where A is the Porod constant, related to the internal surface: volume ratio, and B is the corresponding intensity due to electronic density fluctuation. This positive deviation is related to the surface roughness of the solid network. The intensity contribution, B , is subtracted from the experimental data in order to evaluate the integrated intensity, Q_0 , and total intensity, Q_1 , from the relationships

$$Q_0 = \int_0^\infty q^2 I(q) dq \quad \text{and} \quad Q_1 = \int_0^\infty q I(q) dq.$$

Then the mean chord length produced by the scattering centres is calculated from the relationship

$$l_c = \pi(Q_1/Q_0),$$

which may be considered as the weighted average length of both phases. This parameter represents the harmonic average of the pore and solid chord

$$\frac{1}{l_c} = \frac{1}{l_s} + \frac{1}{l_p}.$$

Therefore, l_p can be calculated.

2.3. Aggregation model

The above analysis can be used to build a geometrical model, the only restriction being that it is necessary to consider the same geometry for the pore and the solid phase. In this case, a pore of diameter,

Table 1
Experimental structural parameters from mercury volumetry, BET and SAXS data

$T \pm 10^\circ\text{C}$	$\phi_s \pm 0.01$	$s_{\text{BET}} \pm 5 \text{ (m}^2 \text{ g}^{-1}\text{)}$	$l_s \pm 1 \text{ (\AA)}$	$l_c \pm 1 \text{ (\AA)}$	$l_p \pm 1 \text{ (\AA)}$
<i>L5 aerogel</i>					
300(10 h)	0.30	461	59	46	215
500(10 h)	0.27	533	51	42	233
650(5 h)	0.30	428	64	45	149
770(5 h)	0.33	407	67	50	193
860(5 h)	0.39	277	98	47	90
950(5 h)	0.52	241	113	44	73
1040(0.5 h)	0.69	167	163	52	76
<i>H5 aerogel</i>					
300(10 h)	0.37	407	68	42	112
500(10 h)	0.36	459	59	41	127
650(5 h)	0.37	460	59	43	153
770(5 h)	0.37	412	66	38	89
860(5 h)	0.42	383	71	40	89
1040(0.5 h)	0.73	238	115	40	62

l_p , can be taken, formed by the aggregation of N_s elementary particles of diameter, l_s , that make up the pore. The solid volume fraction occupied by this distribution will then be

$$\Phi_s = N_s(l_s/l_p)^3.$$

N_s normally refers to the packing coordination number. However, in this proposed model, the particles are not necessarily in contact, thus giving information about the degree of connectivity of the solid network. If, instead of this model, the solid backbone shows internal porosity, the above relationship will

give us a solid cluster, l_s , containing N_p pores whose size is l_p , so the pore volume fraction is

$$\Phi_p = N_p(l_p/l_s)^3.$$

Note the change of the size ratios as to the previous Φ_s expression.

3. Results

Table 1 shows various structural parameters for aerogels L5 and H5. The first column specifies the thermal treatment for each sample, while the second gives the results for the solid volume fraction as the quotient of the bulk and skeletal silica densities. The former is calculated by mercury volumetry with an estimated error of 5% and the latter is the experimental value for glass silica (2.2 g cm^{-3}). As can be seen, there is an increase in the solid phase with temperature. The solid clusters run parallel to a decrease in the specific surface area (column 3) that gives the necessary energy for viscous flow. It is worth noting that a greater decrease is obtained for the L5 sample than for the H5 sample.

Column 4 shows the values of l_s from Eq. (1), while columns 5 and 6 give the values from the chord analysis using the expressions in Section 2.2. The results explain the sintering process on heating, which is more important in the L5 sample. For some

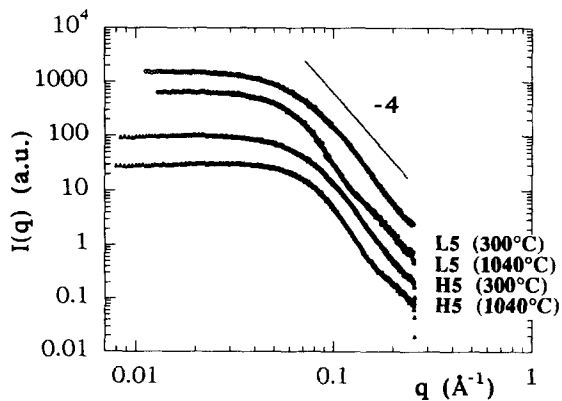


Fig. 1. Log I –log q SAXS curves for L5 and H5 aerogels. The last heat treatment (1040°C–30 min) is plotted to show the change in the high q -region (inflection point).

of the aerogels, the l_c values were calculated from the experimental intensities shown in Fig. 1, using a $\log I - \log q$ plot. The curves yield Porod slopes close to -4 , but there is evidence of single-sphere scattering superimposed on this slope, causing a portion of the curve to have less than -4 , around an inflection point at $\sim 0.15 \text{ \AA}^{-1}$. As can be seen, the results for l_c do not disagree in terms of the regular plateau shown by all of the samples in the low q -region of the $\log I - \log q$ plot, which is a characteristic of the very homogeneous distribution of scattering centres. Note the lower values for the H5 sample.

The trends in both the pore and solid chord values change at a temperature around 770°C for the L5 sample, whereas for the H5 sample the change takes place around 860°C . On the other hand, the net growth of the solid phase for the L5 sample is 2.2 times larger than that for H5, and the pore collapse is 2.8 times faster for L5. These results are in agree-

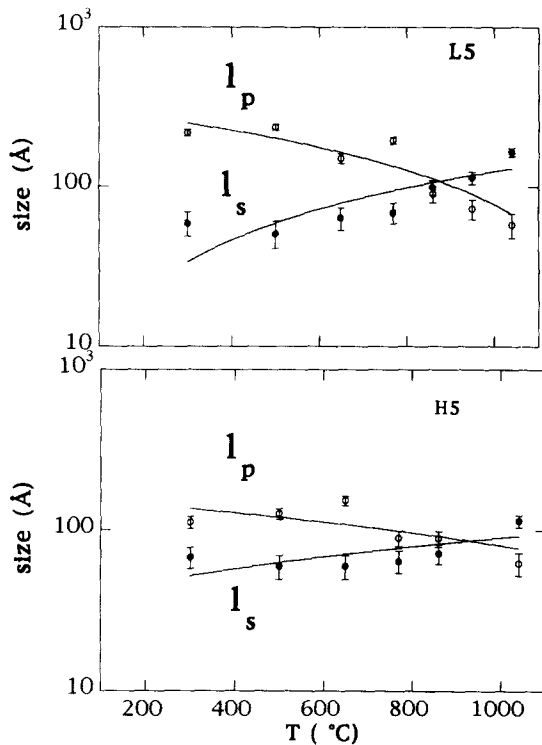


Fig. 2. Size of the pore and solid chords from Table 1 as a function of the treatment temperature. The lines are a guide to the eye.

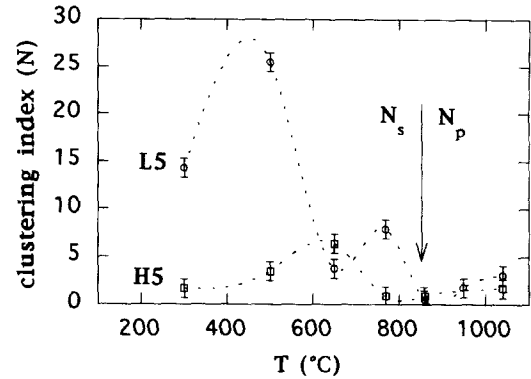


Fig. 3. Clustering index calculated from the relationships in Section 2.3. The dotted lines are a guide to the eye.

ment with the lower l_c -values for the H5 sample. In order to see the above results more clearly, they are plotted in Fig. 2, indicating the point where the hierarchy change from pores to solid takes place.

Fig. 3 shows the behaviour of the calculated clustering index, N , for both aerogels as obtained from the expressions in Section 2.3. As can be seen, the higher values correspond to sample L5 (low ultrasonic dose). The H5 (high ultrasonic dose) sample with lower N values sinters more slowly.

4. Discussion

Ultrasonic treatment in the liquid state influences the thermal behaviour of the aerogels. The higher specific surface area of the L5 sample gives rise to sintering which, from the results the interfacial energy supplies, can be estimated as 1.74 times faster. The low ultrasonic dose treatment facilitates the aggregation process, because the collapse of the pores begins at a lower temperature than that for a high ultrasonic dose.

In Fig. 1, the inflection point indicates the spherical shape of the scattering centres, and its shift for the heat-treated samples (1040°C) reveals a smoothing of the pore-solid boundary as well as a decrease in sphere size, in agreement with the values calculated for l_c . The lower l_c -values for the H5 sample are the result of the cavitation effect of the ultrasound.

The values of the clustering index (Fig. 3), which is the parameter that account for the packing level,

reveal that the geometrical model with a variable hierarchical ratio gives information concerning the structural change on sintering. The increase in N at 500°C is due to the curing treatment producing a smoothing of the pore–solid boundary by removing organic residuals, so that the nitrogen has a more accessible surface. The results explain the aggregation process on heating; first the aerogels sinter by coalescence of the solid phase, but when they reach about 50% of the final density, the collapse of pores is the main sintering mechanism.

5. Conclusions

The sintering process for aerogels can be modeled by means of a hierarchical structure formed by the aggregation of elementary silica spheres. The network connectivity on heating is monitored by the pore to solid size ratio. The viscous flow forms colloidal-like clusters with internal porosity, the collapse of which gives the final monolithic silica glass.

A low ultrasonic dose sample (L5) yields an aggregation level which allows faster sintering at lower temperature than a high ultrasonic dose sample (H5). This is mainly due to the coalescence of the smaller particles, which gives rise to a higher interfacial energy for the viscous flow. In the 700–800°C temperature range, a change takes place in the hierar-

chical level, the collapse of the pores now being the sintering mechanism.

This work has been supported by the CICYT (Comisión Interministerial de Ciencia y Tecnología), under the project MAT91-1022.

References

- [1] J. Zarzycki, M. Prassas and J. Phalippou, *J. Mater. Sci.* 17 (1982) 3371.
- [2] S. Wallace and L.L. Hench, in: *Better Ceramics Through Chemistry*, ed. C.J. Brinker, D.E. Clark and D.R. Ulrich (Elsevier, New York, 1984) p. 47.
- [3] J. Fricke, in: *Aerogels* (Springer, Berlin, 1986) p. 127.
- [4] S.R. Su and P.I.K. Onorato, in: *Better Ceramics Through Chemistry II*, ed. C.J. Brinker, D.E. Clark and D.R. Ulrich (North-Holland, New York, 1986) p. 237.
- [5] T. Lours, J. Zarzycki, A. Craievich, M. Aegerter and D. dos Santos, *J. Non-Cryst. Solids* 106 (1988) 157.
- [6] N. de la Rosa-Fox, L. Esquivias, A. Craievich and J. Zarzycki, *J. Non-Cryst. Solids* 121 (1990) 211.
- [7] N. de la Rosa-Fox, L. Esquivias and J. Zarzycki, *Diff. Defect Data* 53&54 (1987) 363.
- [8] N. de la Rosa-Fox, M.C. Barrera-Solano and L. Esquivias, *J. Non-Cryst. Solids* 147&148 (1992) 58.
- [9] J. Zarzycki, *J. Non-Cryst. Solids* 121 (1990) 110.
- [10] N. de la Rosa-Fox, L. Esquivias, J. Zarzycki and A. Craievich, *Riv. Staz. Sper. Vetro* I-20 (5) (1990) 67.
- [11] G. Porod in: *Small Angle X-Ray Scattering*, ed. O. Glatter and O. Kratky (Academic Press, London, 1982) p. 17.
- [12] W. Ruland, *J. Appl. Crystallogr.* 4 (1971) 70.